Molecular dynamics simulations of structural instability of fullerene family under tension force

Razie Izadi, Ali Nayebi*, Esmaeal Ghavanloo

School of Mechanical Engineering, Shiraz University, Shiraz 71963-16548, Iran

Abstract

Fullerene molecules are cage-like nanoscopic structures with pentagonal and hexagonal faces. In practical applications such as fullerene-reinforced nanocomposites (FRNCs), these structures may be subjected to tension force. In this research, we employ molecular dynamics (MD) simulation to compute the behavior and deformation of different fullerene molecules, ranging from C_{60} to C_{2000}, under tension force. To model the interactions between carbon atoms in the MD simulations, the adaptive intermolecular reactive bond order (AIREBO) force field is used. The displacement-force and the displacement-strain energy curves are obtained. It is observed that a new type of structural instability occurs in the fullerene molecules when the applied tension force increases. This abnormal structural instability in the fullerenes is investigated for the first time in the literature. The critical tensile forces and the corresponding mode shapes are determined for different fullerenes. The results indicate that the critical forces and deformations strongly depend upon the number of carbon atoms.

Key words: Fullerene; Structural instability; Molecular dynamics simulation

1. Introduction

The discovery of a new solid carbon molecule with great stability, so-called fullerene, in 1985 considerably extended the scope and variety of carbon molecules and has opened an entirely new chapter on the physics and chemistry of carbon, with many potential applications [1]. Fullerene molecules are considered as icosahedral closed cage of carbon atoms where the atoms approximately lie either on the surface of a sphere or on the surface of a spheroid. This class of nanoscopic structures is usually denoted by C_N, where N is the number of carbon atoms. C_{60}

* Corresponding author.

Tel.: +98-7136133029, Fax: +98 7136473511

E-mail: nayebi@shirazu.ac.ir (A. Nayebi)

fullerene is the first stable member of the fullerene family. All members of fullerene family consist of an arbitrary number of hexagonal faces and precisely 12 pentagonal faces which play the major role in forming the curvatures of the fullerenes. In hexagonal or pentagonal faces each carbon atom is bonded to three nearest neighbor carbon atoms via sp^2 hybridized bonds [2] with an average carbon-carbon distance of 1.44 Å [3]. Since these molecules have unique physical properties, they have numerous applications which include incorporation into polymers to reinforce the nanocomposites [4-6], incorporation into thin films, and the design of novel electronic devices [2]. Furthermore, fullerenes have also been selected for potential uses in medicine applications [7, 8]. Their closed geodesic structures can also use as a drug delivery carrier [9]. In addition, their pseudo-spherical shape and the weak van der Waals interaction between fullerene molecules and surrounding medium make fullerenes good candidates for nano-bearings with super low friction [10].Therefore, the mechanical properties and behavior of fullerene family have been investigated by several researchers.

The first effort in the mechanical modeling of fullerene molecule was carried out by Ruoff and Ruoff [11]. They estimated the bulk modulus of an individual C_{60} molecule and its single crystal. A further study later published by the same group [12] to improve their previous estimation by adopting a molecular modeling approach. Shen [13] performed molecular dynamics (MD) simulations to investigate the compressive mechanical properties of C_{60} and endohedral fullerene $M@C_{60}$ (M=Si, Ge) molecules at different temperatures. Giannopoulos et al. [14] used a molecular mechanics approach in order to study the radial elastic stiffness and vibrational characteristics of different fullerenes including C_{20}, C_{60}, C_{80}, C_{180}, C_{260}, C_{320}, C_{500} and C_{720} molecules. In another study, Todt et al. [15] estimated the mechanical properties of fullerenes on the basis of continuum shell models and Monte Carlo (MC) simulation. Recently, elastic modulus of the C_{60} molecule was predicted by Jamal-Omidi et al. [16] using the finite element method. More recently, a new approach has been designed to estimate Young's modulus of different spherical fullerenes by combining MD simulations and continuum shell theory [17].

Furthermore, different modeling investigations have been carried out to characterize the vibrational behavior of these nanoscopic structures. The axisymmetric vibrations of fullerene C_{60} have been predicted by Chadderton [18] on the basis of thin elastic shell model. Behfar and Naghdabadi [19] studied the vibrational analysis of multi-shell fullerene embedded in an elastic medium by using the continuum method. Adhikari and Chowdhury [20] investigated the natural the natural frequency and vibration modes of fullerene family on the basis of the molecular mechanics simulation. In In another theoretical study using the finite element method, vibrational analysis of C_{60}

and C_{30} fullerenes has been performed [21]. On the basis of nonlocal elasticity theory, Ghavanloo and Fazelzadeh [22] studied axisymmetric vibration of spherical shell-like nanostructures including the spherical fullerenes and empty spherical viruses. Recently, the natural frequencies of C_{60} have been calculated by Nejat Pishkenari and Ghaf Ghanbari [23] using MD simulations with seven bond-order potentials and five force fields.

In recent years, fullerene-reinforced nanocomposites (FRNCs) have attracted considerable attention among the community of scientific researchers [24-27]. In the FRNCs, due to the sensible difference between the stiffness of the fullerene and the matrix, the fullerenes may be subjected to tension force. Despite the importance of this phenomena, to the authors' knowledge, no investigation has focused sufficiently on the behavior and deformation of fullerenes under tension forces. Hence, in this investigation, we present a comprehensive study to investigate the mechanical behavior of fullerenes when subjected to tensile loading and the feasibility of structural instability. In this way, the mechanical behavior of several icosahedral fullerenes ranging from C_{60} to C_{2000} is investigated. Accordingly, this study performs the MD simulations based on the Adaptive Intermolecular Reactive Empirical Bond Order (AIREBO) [28] force field to model the interactions among carbon atoms. Here, all simulations are performed at 1 K. It is the first reported attempt to use MD simulations to investigate the deformation and structural instability of fullerene molecules.

2. Simulation details

In the present paper, all MD simulations are performed using the large scale atomic/molecular massively parallel simulator (LAMMPS) [29] and VMD package [30] is employed to visualization of the results. Since choosing an appropriate interatomic potential is very important to obtain reasonable results with sufficient precision, the AIREBO potential function is adapted to model the interactions among carbon atoms in the fullerenes. The AIREBO potential is able to accurately reproduce the mechanical behavior observed experimentally in the fullerenes [23]. This potential function consists of three sub-potentials, which are the reactive empirical bond order (REBO) potential E^{REBO}, the Lennard-Jones potential E^{LJ}, and torsional potential E^{Tors}. Two first potentials are pairwise potentials while the last one is four-body interatomic potential function. The AIREBO potential function is defined mathematically as [31, 32]

$$E_{AIREBO} = \frac{1}{2}\sum_{i}^{N}\sum_{j\neq i}^{N}\left(E_{ij}^{REBO} + E_{ij}^{LJ} + \sum_{k\neq i,\, j\neq i,\, j,k}^{N}\sum E_{kijl}^{Tors}\right) \quad (1)$$

To reduce the computational effort, all of the simulations are done with the cut-off distance 12.20 Å. In order to simulate the tensile test, the initial geometry of fullerene molecules is first created in LAMMPS. Prior to deformation, the initial geometry of molecules is relaxed to achieve a stress-free state and minimum energy by using the conjugate gradient algorithm. After initial energy minimization, the canonical ensemble NVT, in which the fixed variables are the number of atoms, volume and temperature, is applied. Furthermore, to maintain the simulation temperature at 1 K, the Nosé–Hoover thermostat algorithm [33] is used and the velocity Verlet algorithm [34] is applied to perform numerical integrations with simulation time-step 1 fs.

In the present simulations, each fullerene molecule is divided into three regions, depending on the boundary conditions imposed (Fig. 1). The first region consists of the lowermost hexagonal face where all atoms are kept fixed (black color). The atoms of the uppermost hexagonal face (second region) are constrained to move along the *z*-axis (red color). In the third region, the atoms are allowed to move freely. Furthermore, the lowermost and uppermost hexagonal faces are exactly opposite to each other and are not destroyed during the simulation. In addition, to study the deformation of the fullerene, we perform uniaxial tensile tests under deformation-control method. The deformation rate is set to 0.01 Å/s which is verified to be small enough to ensure quasi-static deformation. The tensile force exerted on the fullerene is computed by the summation of inter-atomic forces between carbon atoms of the uppermost hexagonal face. Thus, if the *z*-axis is assumed to lie along the displacement direction of the fullerene, then axial force (F) is computed as follows:

$$F = \sum_{i=1}^{6} F_{Zi} \tag{2}$$

where F_{Zi} is the component of inter-atomic forces along the *z*-axis.

3. Results and discussion

In the present study, the onset of structural instability in the fullerene is identified by a sudden/sharp drop in the strain energy as well as the axial force caused by the abrupt changes in structural configurations. The similar criterion have been widely used in the literature to determine the buckling in carbon nanotubes [35-40]. To interpret the observation of the instability in the fullerenes, it should be noted that the tensile forces applied at the upper hexagonal face of the fullerenes leads to the circumferential compressive stress. Under this compressive stress, the distance between atoms in equatorial region of the fullerene reduces and consequently the interatomic forces

increases. As the group of atoms come too close to each other a relative slip will occur especially in equatorial region and the atoms form a new configuration to endure smaller interatomic forces. This leads to a sudden drop in the axial force as well as the strain energy.

From the MD simulations, the displacement of the upper hexagonal, the tensile force and the strain energy due to the applied force are directly computed, and then the force-displacement curve and the strain energy curve are plotted. Typical force-displacement curve for C_{540} is shown in Fig. 2a. The maximum force before the initiation of instability is termed the critical force (F_{cr}), while the corresponding elongation is termed the critical displacement (Δ_{cr}). As it is shown, the force drops suddenly at displacement 7.1 Å with a critical force F_{cr} = 52.9 nN (point B in the Fig. 2). Furthermore, it is observed that the force-displacement curve is approximately linear prior to the onset of instability. To ensure the occurrence of the instability in the fullerene, the strain energy-displacement curve for C_{540} is also plotted in Fig. 3. At a displacement 7.1 Å, a sudden drop in the strain energy is also observed. The drop in force-displacement curve is more observable than the strain energy-displacement curve at the same displacement. Noted that, the sudden energy release and the corresponding drop in force are associated with significant structural and geometrical changes of fullerene molecules. As it can be seen in Fig. 3, the strain energy varied quadratically in term of the displacement. Furthermore, the loading-unloading curves are plotted in Fig. 4. As it can be seen, the unloading curve retracts along the same path as the loading curve, as shown in Fig. 4. This means that the material behavior before point B is purely elastic.

According to the prescribed criterion, the critical force and corresponding displacement, and the magnitudes of energy release at the critical load are calculated and listed in Table 1 for nine fullerene molecules including C_{60}, C_{180}, C_{240}, C_{540}, C_{720}, C_{980}, C_{1280}, C_{1620} and C_{2000}. As can be inferred from the results in the table, the values of critical displacement increase with respect to increasing the size of the molecules. In addition, Fig. 5 displays the calculated critical force as a function of the equivalent radius of the fullerene. It is apparent from the figure that C_{240} fullerene possesses the maximum force capacity among the investigated cases. It is also observed that, for molecules larger than C_{240}, the critical force decreases with the increase of the molecule size. Finally, the initial and collapsed configurations of the fullerenes are displayed in Fig. 6. In this figure, the snapshots are plotted in *x-y* plane. Furthermore, it should be noted that no bond breaking is occurred during the simulation.

4. Conclusions

A comprehensive molecular dynamic study was conducted for the assessment of structural instability behavior of the nine fullerenes subjected to tensile loading. In this connection, the deformational morphology of the fullerenes was explored via a set of MD-based simulations, employing the AIREBO potential energy function together with the Nosé–Hoover thermostat technique to maintain a constant temperature. The critical force and corresponding displacement were investigated through analyzing the force-displacement and the strain energy-displacement curves obtained from MD simulations. The results obtained indicated that the critical forces and collapsed configurations strongly depend upon the number of carbon atoms. Furthermore, the C_{240} fullerene has maximum force capacity among the simulated fullerenes.

References

[1] H.O. Pierson, Handbook of Carbon, Graphite, Diamonds and Fullerenes: Processing, Properties and applications, Noyes Publications, New Jersey, 1993.

[2] M.S. Dresselhaus, G. Dresselhaus, P.C. Eklund, Science of Fullerenes and Carbon Nanotubes, Academic Press, San Diego, 1996.

[3] D. Baowan, B. J. Cox, T. A. Hilder, J. M. Hill, N. Thamwattana, Modelling and Mechanics of Carbon-based Nanostructured Materials, Elsevier, Cambridge, 2017.

[4] F.J. Balta Calleja, L. Giri, T. Asano, Structure and mechanical properties of polyethylene-fullerene composites, J. Mater. Sci. 31 (1996) 5153-5157.

[5] T. Ogasawara, Y. Ishida, T. Kasai, Mechanical properties of carbon fiber/fullerene-dispersed epoxy composites, Compos. Sci. Technol. 69 (2009) 2002-2007.

[6] P.G. Prasanthi, G.S. Rao, B.U. Gowd, Mechanical performance of Buckminster fullerene-reinforced composite with interface defects using finite element method through homogenization techniques, Compos. Interfaces 22 (2015) 299-314.

[7] R. Bakry, R.M. Vallant, M. Najam-ul-Haq, M. Rainer, Z. Szabo, C.W. Huck, G.K. Bonn, Medicinal applications of fullerenes, Int. J. Nanomedicine 2 (2007) 639-649.

[8] E. Castro, A.H. Garcia, G. Zavala, L. Echegoyen, Fullerenes in biology and medicine, J. Mater. Chem. B 5(2017) 6523-6535.

[9] A. Montellano, T. Da Ros, A. Bianco, M. Prato, Fullerene C_{60} as a multifunctional system for drug and gene delivery, Nanoscale 3 (2011) 4035-4041.

[10] J.W. Kang, H.J. Hwang, Fullerene nano ball bearings: an atomistic study, Nanotechnology 15 (2004) 614-621.

[11] R.S. Ruoff, A.L. Ruoff, Is C_{60} stiffer than diamond?, Nature 350 (1991) 663-664.

[12] R.S. Ruoff, A.L. Ruoff, The bulk modulus of C_{60} molecules and crystals: a molecular mechanics approach, Appl. Phys. Lett. 59 (1991) 1553-1555.

[13] H. Shen, The compressive mechanical properties of C_{60} and endohedral $M@C_{60}$ (M=Si, Ge) fullerene molecules, Mater. Lett. 60 (2006) 2050-2054.

[14] G.I. Giannopoulos, S.K. Georgantzinos, P.A. Kakavas, N.K. Anifantis, Radial stiffness and natural frequencies of fullerenes via a structural mechanics spring-based method, Fuller. Nanotub. Car. N. 21 (2013) 248-257.

[15] M. Todt, F.G. Rammerstorfer, Continuum shell models for closed cage carbon nanoparticles, in: W. Pietraszkiewicz, J. Gorski (Eds.), Shell Structures: Theory and Applications 3 (2014) 149-152.

[16] M. Jamal-Omidi, M. ShayanMehr, R. Rafiee, A Study on equivalent spherical structure of buckyball-C_{60} based on continuum shell model, Lat. Am. J. Solids Struct. 13 (2016) 1016-1029.

[17] E. Ghavanloo, R. Izadi, A. Nayebi, Computational modeling of the effective Young's modulus values of fullerene molecules: a combined molecular dynamics simulation and continuum shell model, J. Mol. Model. 24 (2018) 71.

[18] L. T. Chadderton, Axisymmetric vibrational modes of fullerene C_{60}, J. Phys. Chem. Solids 54 (1993) 1027-1033.

[19] S. K. Behfar, R. Naghdabadi, Nanoscale modeling of an embedded multi-shell fullerene and its application to vibrational analysis, Int. J. Eng. Sci. 44 (2006) 1156-1163.

[20] S. Adhikari, R. Chowdhury, Vibration spectra of fullerene family, Phys. Lett. A 375 (2011) 2166-2170.

[21] J.H. Lee, B.S. Lee, F.T.K. Au, J. Zhang, Y. Zeng, Vibrational and dynamic analysis of C_{60} and C_{30} fullerenes using FEM, Comput. Mater. Sci. 56 (2012) 131-140.

[22] E. Ghavanloo, S. A. Fazelzadeh, Nonlocal shell model for predicting axisymmetric vibration of spherical shell-like nanostructures, Mech. Adv. Mater. Struc. 22 (2014) 597-603.

[23] H. Nejat Pishkenari, P. Ghaf Ghanbari, Vibrational properties of C_{60}: a comparison among different inter-atomic potentials, Comput. Mater. Sci. 122 (2016) 38-45.

[24] A. Adnan, C.T. Sun, H. Mahfuz, A molecular dynamics simulation study to investigate the effect of filler size on elastic properties of polymer nanocomposites, Compos. Sci. Technol. 67 (2007) 348-356.

[25] P. Prasanthi, G.S. Rao, B.U. Gowd, Effectiveness of buckminster fullerene reinforcement on mechanical properties of FRP composites, Procedia Mater. Sci. 6 (2014) 1243-1252.

[26] F. Jeyranpour, G. Alahyarizadeh, H. Minuchehr, The thermo-mechanical properties estimation of fullerene-reinforced resin epoxy composites by molecular dynamics simulation- a comparative study, Polymer 88 (2016) 9-18.

[27] C.T. Lu, A. Weerasinghe, D. Maroudas, A. Ramasubramaniam. A comparison of the elastic properties of graphene- and fullerene-reinforced polymer composites: the role of filler morphology and size, Sci. Rep. 6 (2016) 31735.

[28] S. J. Stuart, A. B. Tutein, J. A. Harrison, A reactive potential for hydrocarbons with intermolecular interactions, J. Chem. Phys. 112 (2000) 6472-6486.

[29] P. Steve, P. Crozier, A. Thompson, LAMMPS-large-scale atomic/molecular massively parallel simulator, Sandia Nat. Lab. 18 (2007) 43.

[30] W. Humphrey, A. Dalke, K. Schulten, VMD: visual molecular dynamics, J. Mol. Graph. 14 (1996) 33-38.

[31] S.J. Stuart, A.B. Tutein, J.A. Harrison, A reactive potential for hydrocarbons with intermolecular interactions, J. Chem. Phys. 112 (2000) 6472-6486.

[32] A. Montazeri, S. Ebrahimi, H. Rafii-Tabar, A molecular dynamics investigation of buckling behaviour of hydrogenated graphene, Mol. Simul. 41 (2015) 1212-1218.

[33] S. Nosé, A unified formulation of the constant temperature molecular dynamics methods, J. Chem. Phys. 81 (1984) 511-519

[34] M.P. Allen, D.J. Tildesley, Computer Simulation of Liquids, Clarendon Press, Oxford, 1987.

[35] H.W. Zhang, K. Cai, L. Wang, Deformation of single-walled carbon nanotubes under large axial strains, Mater. Lett. 62 (2008) 3940-3943.

[36] C.H. Wong, V. Vijayaraghavan, Nanomechanics of imperfectly straight single walled carbon nanotubes under axial compression by using molecular dynamics simulation, Comput. Mater. Sci. 53 (2012) 268-277.

[37] B. Motevalli, A. Montazeri, R. Tavakoli-Darestani, H. Rafii-Tabar, Modeling the buckling behavior of carbon nanotubes under simultaneous combination of compressive and torsional loads, Physica E 46 (2012) 139-148.

[38] S.C. Chowdhury, B.Z. Haque, J.W. Gillespie, D.R. Hartman, Molecular simulations of pristine and defective carbon nanotubes under monotonic and combined loading, Comput. Mater. Sci. 65 (2012) 133-143.

[39] S.S. Gupta, P. Agrawal, R.C. Batra, Buckling of single-walled carbon nanotubes using two criteria, J. Appl. Phys. 119 (2016) 245106.

[40]. Z.K.J. Kok, C.H. Wong, Molecular dynamics simulation studies of mechanical properties of different carbon nanotube systems, Mol. Simul. 42 (2016) 1274-1280.

Table 1. Critical force and displacement, and the magnitudes of energy release at the critical load for different fullerenes

Fullerene	F_{cr} (nN)	Δ_{cr} (Å)	ΔE(eV)
C_{60}	56.2	2.1	0.8
C_{180}	72.4	5.3	7.8
C_{240}	84.4	6.3	23.6
C_{540}	52.9	7.1	13.6
C_{720}	44.7	6.5	0.2
C_{980}	40.6	7.4	0.4
C_{1280}	36.2	7.3	0.6
C_{1620}	32.0	7.8	0.3
C_{2000}	27.4	7.8	0.1

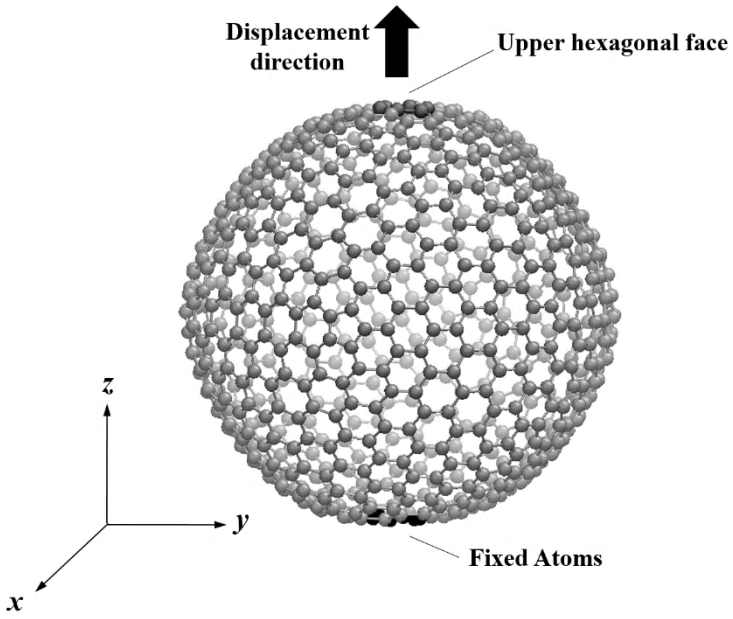

Fig. 1. Molecular structure of C_{720} fullerene subjected to tensile load

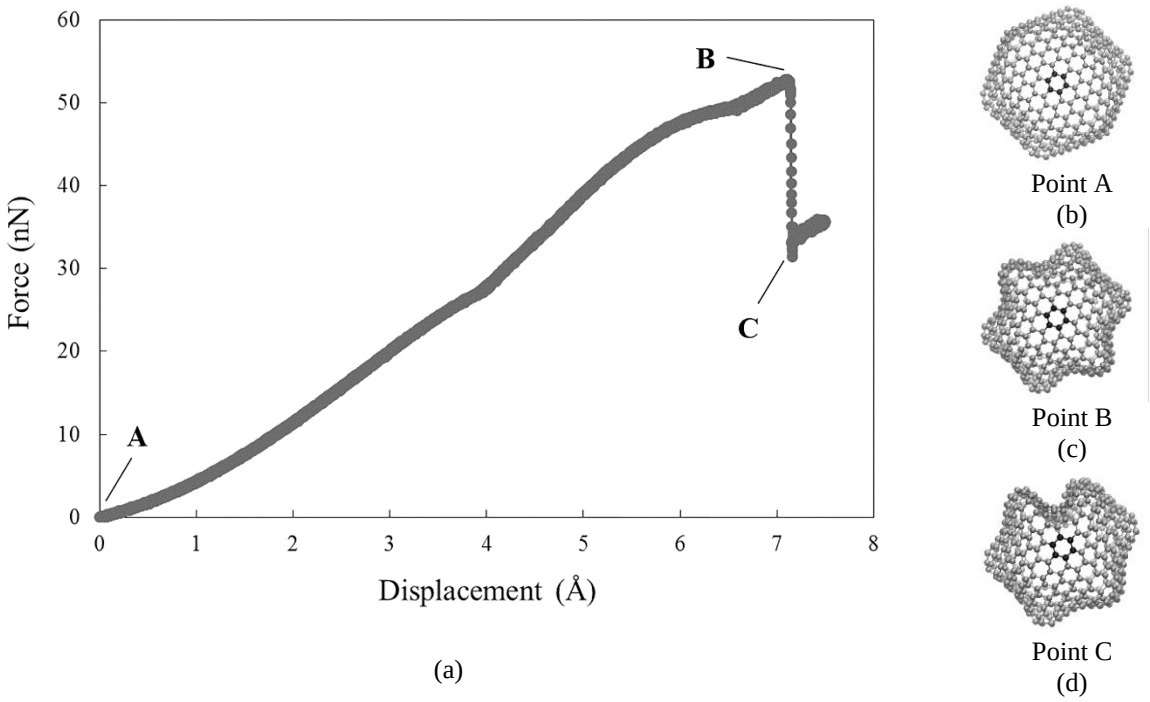

(a)

Fig. 2. (a) Force-displacement curve for C_{540}, (b) Undeformed configuration (point A), (c) deformed configuration prior to the instability (point B) and (d) collapsed configuration (point C).

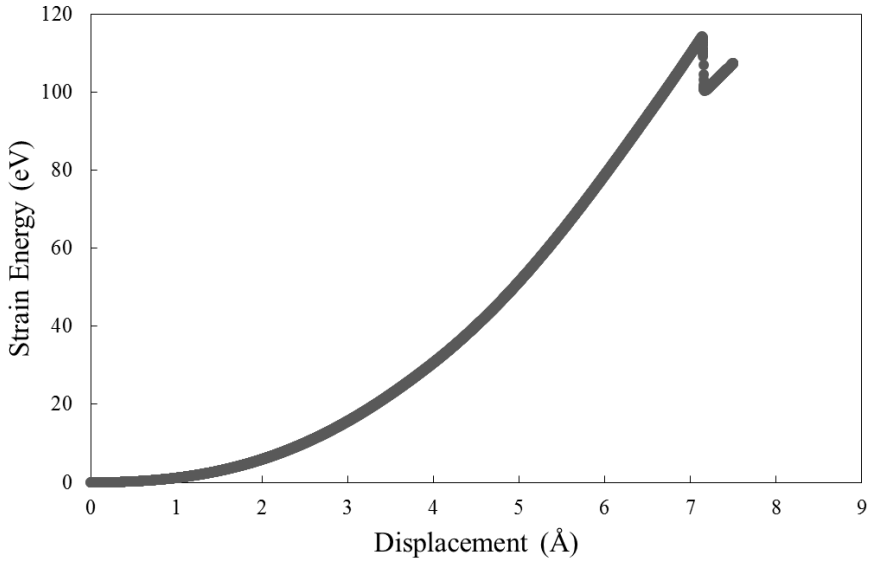

Fig. 3. Strain energy-displacement curve for C_{540}

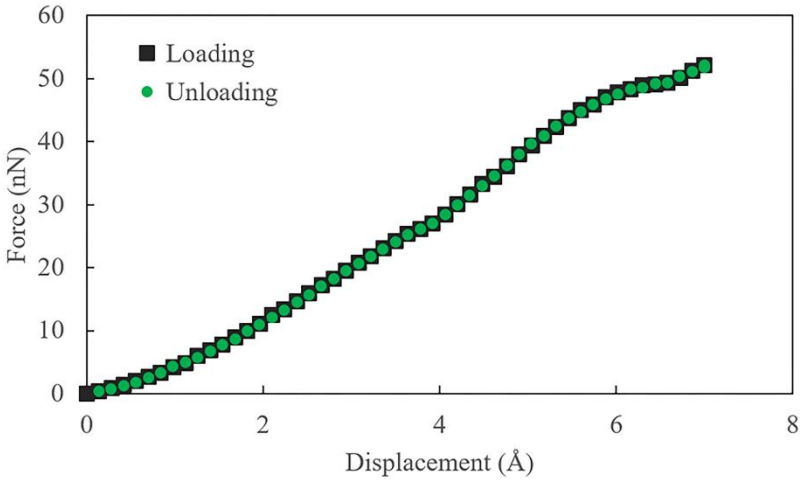

Fig. 4. The loading-unloading curves for C_{540}

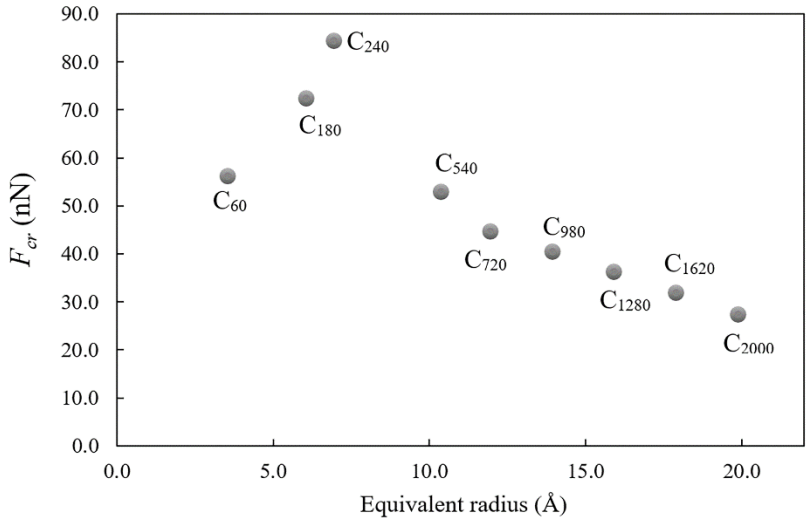

Fig. 5. Variation of the critical force as function of equivalent radius of the fullerene molecules

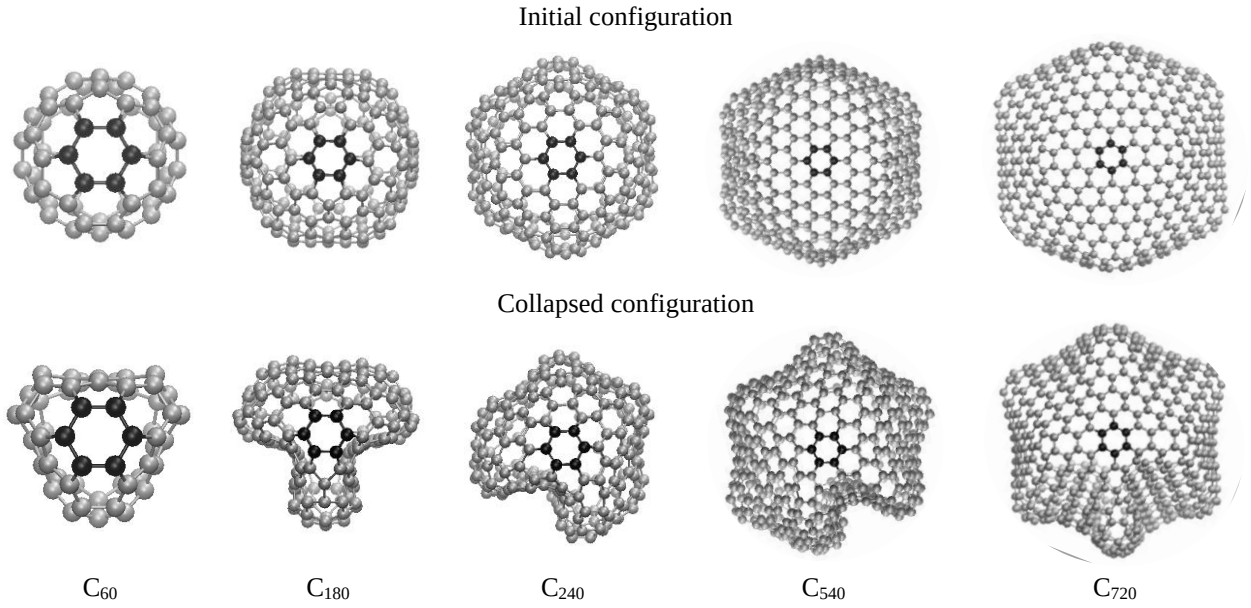

Fig. 6. Initial and collapsed configurations of the nine fullerenes.